CHAPTER 4

FLUID INCLUSION STUDIES

4.1 Introduction

4.1.1 Background

Before describing fluid inclusion studies of samples from the Serra do Navio deposit, an introduction is given to the general principles of fluid inclusions, common fluid inclusions as well as their application in the study of metamorphic rocks.

The study of fluid inclusions in rocks and minerals goes back almost 1000 years. While fluid inclusions were first observed by ancient Greek and Roman scientists (Leeder et al., 1987) it was only in the 11th century that they were described (Roedder, 1984). Since then many scholars reported the presence of bubbles in minerals, the nature of the inclusions, compositions and the basic fluid dynamics (Roedder, 1984). It was only in the mid 1800's however, that Henry C. Sorby published detailed descriptions and interpretations of fluid inclusions (Roedder, 1984). But the use of fluid inclusions in scientific studies remained unfashionable until 40 years ago when interest was revived. Today various types of fluid inclusions in minerals have become an invaluable tool in the study of metamorphic and igneous petrology, ore deposits as well as in petroleum geology.

4.1.2 Basic Principles

Fluid inclusions are small quantities of fluid, usually 5 - 30μm along the longest axis, (liquid and/or vapor) trapped in mostly small cavities within minerals (Van den Kerkhof et al., 1984). The basic reason for fluid inclusion studies is to constrain physico-chemical parameters, most notably of pressure and temperature (P – T), as well as fluid chemistry during trapping. However, the rock may still have a completely different P– T evolution as fluid inclusion contents are seldom inert, and may have been subjected to post-trapping

changes. In sedimentary environments, for example, the inclusions may be altered during diagenetic processes (e.g. Goldstein, 2001). So any fluid inclusion study needs to ascertain that there has not been any leakage, volume or compositional changes at any stage in the P – T evolution of the system. Fluid inclusions must therefore follow a univariant isochoric – isoplethic path in P – T space. This path of constant density (or molar volume) is called an isochore (Fig. 4.1).

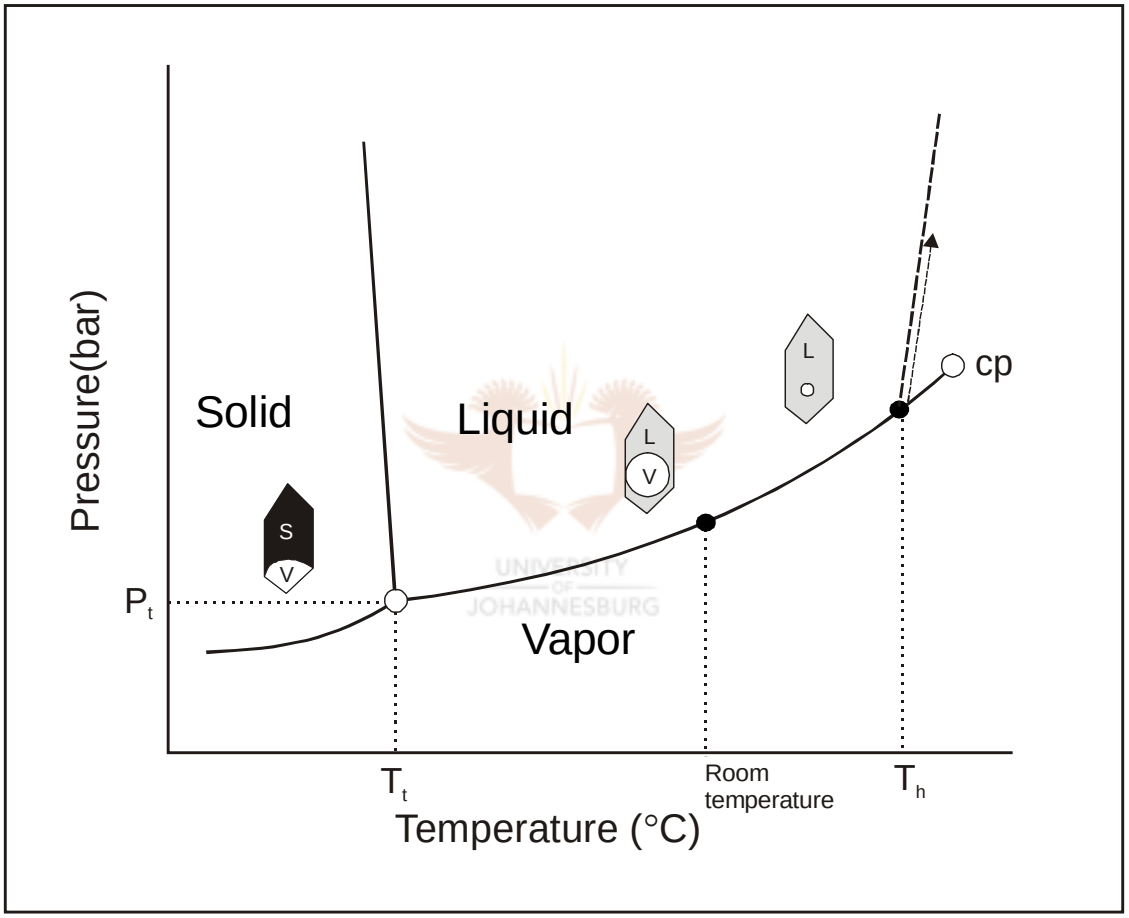

Fig. 4.1: The P – T evolution of an aqueous fluid inclusion trapped at some pressure and temperature, then subsequently cooled down along a path of constant density (or molar volume, i.e. an isochore. S = Solid, L = Liquid, V = Vapor, Th = homogenization temperature, Pt – Tt = Pressure and temperature at the Triple point of water; cp = critical point.

Fluid inclusions occur in many rock-forming minerals from most terrestrial environments. Theoretically almost all minerals can be studied for fluid inclusions. However features like color, mechanical hardness, cleavage and transparency may place

restrictions on which minerals can be comprehensively studied. Quartz is the ideal choice for fluid inclusions in igneous as well as metamorphic rocks particularly because it usually is ubiquitous in nearly all metamorphic rocks and contains the most inclusions. It is also stable at all metamorphic conditions within the crust. It does not react chemically with trapped fluids, in contrast to other minerals that may exchange cations with species dissolved in aqueous inclusions. The absence of cleavage in quartz also prevents fluid inclusions from leaking along cleavage planes.

However, quartz is not always an ideal host mineral for several reasons. It suffers deformation and/or recrystallization most easily over a wide range of P – T conditions. Too many fluid generations may be present making it almost impossible to distinguish between different trapping events. Additionally, no P –T indications can be deduced from quartz itself. So it must consequently be studied with the greatest attention (Van den Kerkhof, 2001) especially relative to other P –T sensitive minerals. Therefore, other minerals that consistently reflect particular P – T conditions, notably garnet, are studied. Other minerals that are also studied for inclusions include fluorite, barite, calcite and gypsum. Fluid inclusions are also studied in ore minerals that are transparent in infrared light e.g. hematite and sphalerite (e.g. Wilkinson, 2001).

The observation of the spatial distribution of different fluid inclusion populations within a mineral grain is of great importance in establishing their paragenetic successions relative to mineral formation. Three fundamental types of fluid inclusions are identified: isolated inclusions, inclusion clusters and inclusion trails (Roedder, 1984). The first two are generally accepted to be of primary origin. Primary fluid inclusions are incorporated during crystal growth (Lemmlein, 1956). These inclusions occur in minerals that grew in an environment with a free fluid phase. The third, however, reflects micro crack healing subsequent to mineral growth. These belong to secondary inclusions that form by sealing of fluid filled fractures in minerals. The walls of these fractures grew together isolating small pockets of the fluid that had entered the open cracks. Secondary inclusions along healed cracks form after the mineral grain crystallized although in some cases growth could have been proceeding when the crack opened, producing pseudosecondary

inclusions (Ermakov, 1949). It is generally believed that only a few samples are dominated by primary fluid inclusions whereas secondary, pseudosecondary and inclusions of indeterminate age dominate most systems (e.g. Goldstein, 2001). This means that the origin of the trapped fluid and in most cases its relation to mineral formation remains unknown. Both primary and secondary inclusions occur in metamorphic rocks, but conditions of entrapment, their composition and complexities introduced by post-entrapment are different from those in igneous and hydrothermal rocks. This is due to the long time span for metamorphic processes and the fact that the fluid phase never forms more than a minor component in most metamorphic systems.

In the study of ore deposits or metamorphic rocks, often more than one fluid is trapped simultaneously. This poses the question about which of the fluids is the mineralizing one. Observations like these underline the importance of careful petrographic analyses of samples that will be subjected to fluid inclusion studies. This is important as it determines whether the inclusions present are suited to answer the geological questions raised.

4.1.3 Common fluids in metamorphic rocks

Studies of fluid inclusions have documented the variety of fluids present in metamorphic rocks: H_2O, saline, CO_2, CH_4 and N_2. Most inclusions are filled by saline solutions with variable amounts of chlorides (NaCl, KCl, $CaCl_2$) or other salts. Because of the complexities inherent to natural processes, fluids are usually mixtures of the components outlined above. In the Earth's crust and upper mantle evidence abounds that the fluid system is characterized by C – O – H – N – S, in addition to the salts. Sulphur species are usually restricted to specific environments leaving C – O – H – N as the most important volatiles (Van den Kerkhof, 1988).

There is no relation between age of rocks and fluid type for comparable rocks. For example Archean metamorphic rocks may contain exactly the same fluid inclusions as younger rocks of comparable metamorphic grade.

4.1.4 Importance of fluid inclusions and their application in the study of metamorphic rocks

Fluid inclusions have raised important petrologic questions, such as the occurrence of abundant CO_2 in granulite facies as well as the presence of $H_2O - N_2$ in eclogites (Touret, 2001). Theses studies have also demonstrated that fluid immiscibility plays an important role in most metamorphic processes. Fluid inclusions have also yielded important information regarding the nature of hydrothermal deposits and mineralizing systems as well as identifying metamorphic fluids. In metamorphic rocks these inclusions are used to infer P – T conditions at which the inclusions formed and to constrain post – metamorphic P – T paths of metamorphic terranes (Touret, 2001). Fluid inclusion studies both support and compliment mineralogical and geochemical studies in determining the evolution of metamorphic terranes.

Information of the P – T conditions at which an inclusion or group of inclusions was formed may be inferred from the density of the fluids trapped in the inclusion. The P – T point at which the inclusion becomes a closed constant volume system determines the density for that inclusion. Two main techniques find application in modern fluid inclusion studies: Microthermometry and Raman Spectroscopy. In the study of rocks from the Serra do Navio deposit microthermometry was extensively used.

4.2 Analytical techniques

4.2.1 Sample selection

From a petrographic examination of a suite of 50 samples from the Serra do Navio deposit, three were selected for fluid inclusion studies (Table 4.1). The selection was done on the premise that most of the quartz at the Serra do Navio deposit does not contain fluid inclusions of suitable size for analysis. However, spessartine garnets in the rocks contain suitable and abundant inclusions for analysis. This is a good choice because solid inclusion-free spessartine porphyroblasts give us a well-constrained estimate for metamorphic conditions during their formation. The three selected samples (Table 4.1)

thus defined good examples of solid inclusion-free spessartine porphyroblasts with fluid inclusions.

Table 4.1: The host minerals and associated rock types selected for fluid inclusion studies

Sample	Host mineral	Rock type
DH114-H	Spessartine	Rhodochrosite marble
DH114-M	Spessartine	Rhodochrosite marble
DH140-I	Spessartine	Biotite schist

4.2.2 Microthermometry

Microthermometry is the most commonly used non-destructive analytical technique in the study of fluid inclusions. It is relatively inexpensive and gives the possibility of reliably determining the compositional and physical properties for the trapped phases. Microthermometry involves freezing and heating of inclusions while observing phase changes through a light microscope thereby determining the fluid composition and density.

Modern microthermometry involves both simple heating - freezing runs and sequential heating – freezing runs. The latter often provides a better insight in phase changes or estimation of certain phase proportions in terms of volume % of the inclusion.

In this study samples were doubly polished to ~300µm thick and measurements were done using a Linkam TMH 600 heating/freezing stage. Liquid nitrogen and a thermal resistor are used for cooling and heating, respectively. The heating – freezing stage is mounted on a binocular *Olympus BH 60* infrared microscope with a maximum magnification of 500x. Inclusions were cooled to ~ -120 ˚C and phase transitions were measured upon heating. Using a heat resistant sample holder, the inclusions were heated up to temperatures of ~ 400 ˚C to get the homogenization temperatures.

Calibration of the Linkam stage was done by measuring melting points of pure carbon-dioxide (CO_2, -56.6 ˚C) inclusions hosted by quartz. Homogenization temperatures of the known CO_2 inclusions were used for stage calibration up to 31 ˚C. Measurements of melting temperature T_m and homogenization temperature T_h of the CO_2 inclusions have a precision of +0.2 ˚C.

The temperature measurements that characterize the fluid composition and density of the different fluid types include:

- **Incipient/initial melting temperature (T_{mi})**: the first melting temperature, defined as solid-liquid or solid-vapor to a solid, liquid or vapor phase. This is given by the equation: Ice + Liq + Vap. = Ice + Liq.+ Vap
- **Eutectic melting (T_e)**: first melting for H_2O-NaCl system (-20.8 ˚C). This is given as: Hydrohalite + Liq. + Vap. = Ice + Liq. + Vap.
- **Final melting (T_{mf})**: phase transition from solid, liquid and vapor into liquid and vapor: Ice + Liq + Vap. + Liq + Vap.
- **Clathrate melting (T_{mc})**: melting temperature of gas hydrate: Clathrate + Liq. + Vap. = Liq. + Vap.
- **Homogenization temperature (T_h)**: phase transition from vapor to liquid or liquid to vapor: Liq. + Vap. = Liq.

Fluid composition and molar volume can be estimated from the combination of T_h and T_m (Van den Kerkhof, 1988), especially for binary systems like the ones encountered in this study.

4.3 Results

4.3.1 Fluid Inclusion types and phase transitions

Three principle types of fluid inclusions were identified during microthermometric studies based on their compositions (Table 4.2) namely:

I – Aqueous o H_2O – NaCl inclusions

II – Pure CH_4 inclusions

III – Mixed aqueous H_2O – CH_4 inclusions.

Table 4.2: General characteristics of the fluid inclusion types observed in spessartine at Serra do Navio deposit.

Fluid characteristics	Type 1	Type 2	Type 3
Composition	H_2O – NaCl (0 – 8 wt.% NaCl)	CH_4	CH_4 – H_2O
Host mineral	Spessartine	Spessartine	Spessartine
Density (g/cm^3)	0.73 g/cm^3	~ 0.27 g/cm^3	0.20 – 0.28 g/cm^3

The following phase transitions were observed using microthermometric measurements:

I: H_2O – NaCl system (Fig. 4.2)

- Initial melting of hydrohalite (T_{mi}^{HH}): HH + ice + vapor = liquid + ice + vapor
- Final melting of ice (T_{mf}^{ICE}): ice + liquid + vapor = liquid + vapor
- Homogenization (T_h): liquid + vapor = liquid

II: CH_4 system

- Final melting (Tm): ice + liquid + vapor = liquid + vapor
- Homogenization (Th): liquid + vapor = liquid

III: Mixed CH_4 – H_2O

- Final melting of ice (T_m): ice + liquid +vapor = liquid + vapor
- Clathrate melting (T_{mc}): Clathrate + liquid + vapor = liquid + vapor
- Homogenization (T_h^{AQ}): liquid + vapor = liquid

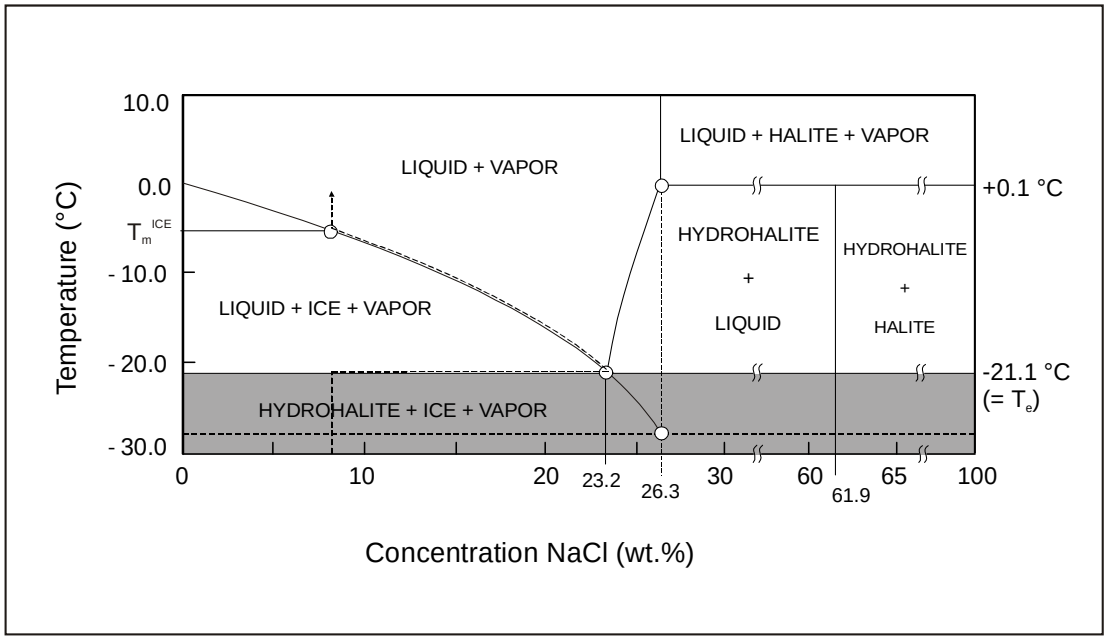

Fig. 4.2: Phase diagram for the system H_2O – NaCl. An aqueous fluid inclusion with a salinity of ~ 8 wt. % NaCl is heated from freezing. This inclusion reaches the invariant eutectic point at –21.1 ºC when all the hydrohalite is consumed. Then it follows the liquidus until the final melting of the ice at about –5 ºC. Note that the salinity determines which fields are entered into at certain phase transitions (modified after Greyling et al., 2001)

4.3.2 Type 1 inclusions: H_2O – NaCl

Liquid – Vapor (LV) inclusions were identified in spessartine. Both isolated and clustered inclusions occur in sample DH114-H and DH114-M, whereas only isolated inclusions are present in DH140-I. Monophase inclusions, consisting of only liquid (L) at room temperature, are scarce. Both LV and L inclusions are colorless – grayish, sometimes elongated and flattened with a spherical bubble sometimes associated with a solid phase (Fig. 4.3). They are usually very small in size, averaging 10µm, even though some infrequent larger ones are present. Microthermometric measurements reveal eutectic temperatures (T_{mi}^{HH}) that range from –29 ºC to –17 ºC. This slight shift from the stable eutectic temperature for the system H_2O – NaCl may indicate metastable eutectic melting (Goldstein and Reynolds, 1994).

High final melting temperatures (T_{mf} ^{ICE}) in monophase inclusions are often attributed to the absence of a vapor phase and a correspondingly low internal pressure (Goldstein and Reynolds, 1994). Homogenization temperatures (T_h) for LV inclusions occurred between 290 ºC and 359 ºC (Fig. 4.4). Final melting temperatures range from –5 to 0ºC (Fig. 4.5). Corresponding salinities vary between 0 wt.% and 8 wt.% NaCl.

4.3.3 Type 2 inclusions: Pure CH_4

These inclusions in spessartine are clear to light gray in appearance. They range in size from 6 - 30μm and they represent about 30% of the inclusions studied. These inclusions are absent from sample DH114-M but infrequent isolated incusions are present in DH114-H. Both isolated and clustered inclusions are present in DH140-I. They are usually irregular in shape and are randomly distributed in spessartine porphyroblasts. Where they occur in clusters they are frequently associated with Type 1 inclusions. Most of these inclusions have both a vapor and liquid phase (LV), but it is not uncommon to see some rare monophase (L) inclusions at room temperature (Fig. 4.3)

Since the melting temperature of pure CH_4 is far below 0 ºC (-182 ºC), it cannot be attained with the heating-freezing stage of the Linkam microscope. As such only the homogenization temperatures characterize these inclusions. The homogenization of these inclusions is always to a liquid state in a wide range of temperatures, from –94 ºC to –83 ºC, just below the triple point of CH_4 (Fig. 4.6). Homogenization temperatures of –91 ºC correspond to a density of ~0.27g/cm^3.

4.3.4 Type 3 inclusion: Mixed $CH_4 – H_2O$

These are the rarest of all the inclusions studied, representing 10% – 13% of the total inclusion population. They are restricted to only sample DH140-I where they exhibit rectangular to rounded shapes, and irregular to negative crystal shapes. They usually range in size between 10 - 30μm. The relative volume of the CH_4 bubble varies between 10% and 50%. The inclusions are usually associated with Type 2 fluid inclusions and

seldom with the Type 1. In one case however they are clustered together with both inclusion types (Fig. 4.3b).

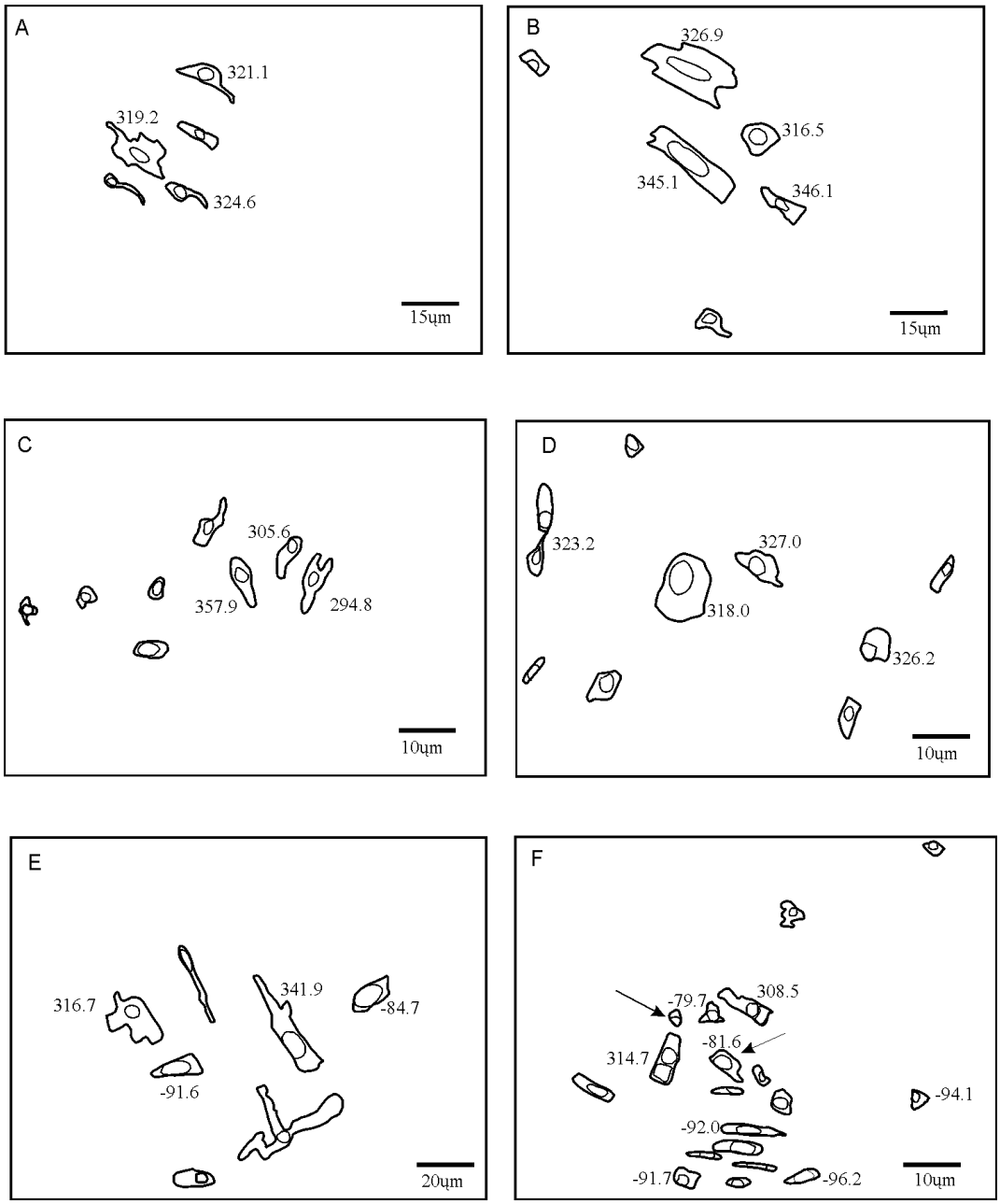

Fig. 4.3a: Sketch of all the 3 inclusions types described with selected homogenization temperatures (ºC). A – D: Type 1 inclusions (H_2O – NaCl) that homogenize above 290ºC (DH114-H and DH114-M)); E – F: Type 2 inclusions (CH_4) with homogenization temperatures above the triple point of pure methane (-82.6 ºC) (DH114-M and DH140-I); F: All inclusion types occurring in proximity to each other, signifying a common origin. The arrows show Type 3 inclusions (CH_4 – H_2O) (DH140-I).

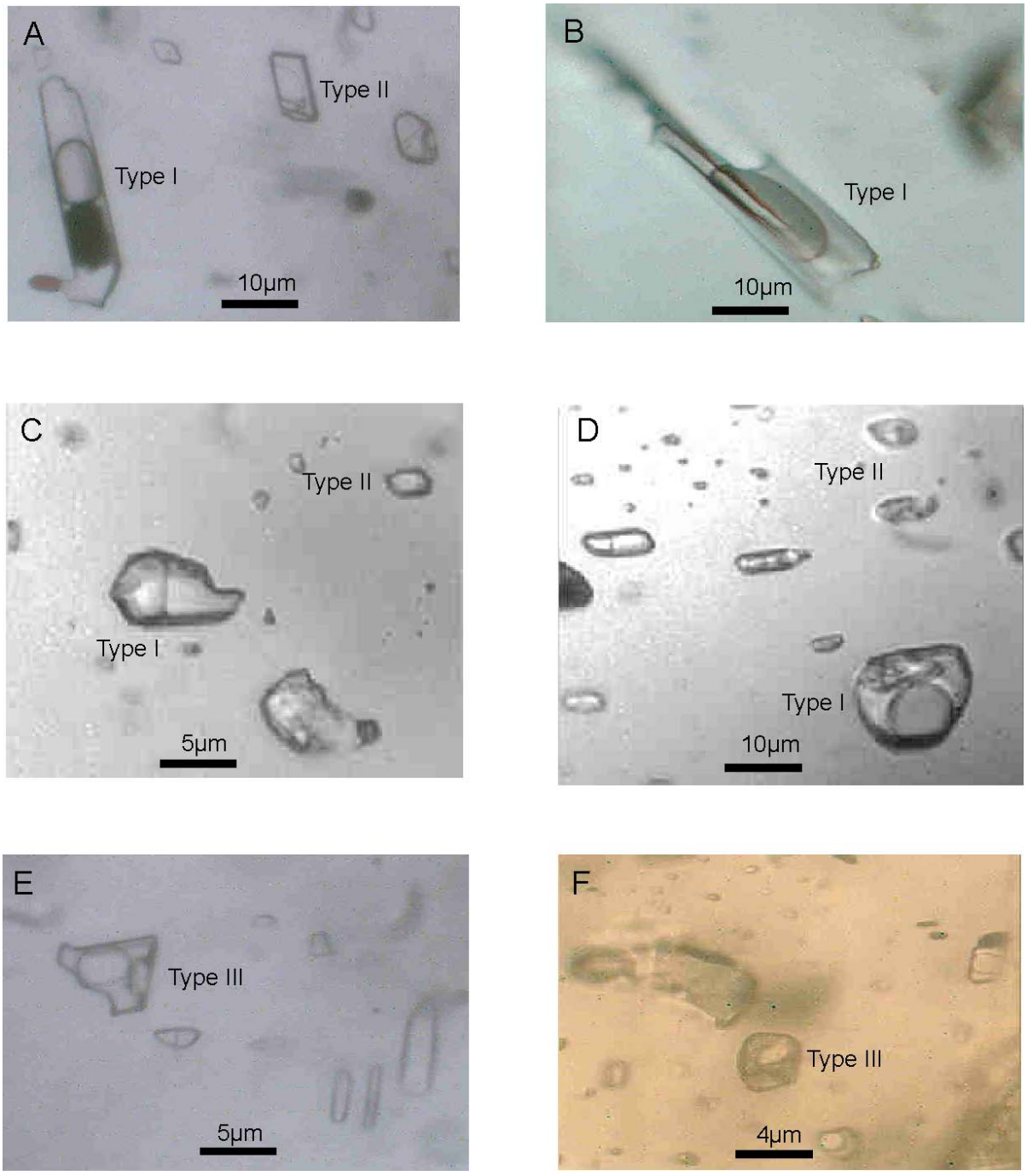

Fig: 4.3b: Typical fluid inclusions identified in spessartine at the Serra do Navio deposit. A and B: Type 1 low-salinity inclusions of the H_2O – NaCl system (DH114-H); C and D: Type 2 inclusion of the pure CH_4 system (DH114-M); E and F: Type 3 mixed inclusions of the CH_4 - H_2O system (DH140-I).

Microthermometry reveals partial homogenization (L. + V. = L) between –82 ºC and –77 ºC (Fig. 4.7). Clathrate dissociation temperatures were recorded between ±10 and ±15 ºC. Total homogenization temperatures were not measured since it is assumed that these inclusions were not homogenous at fluid trapping conditions. These inclusion types originated from heterogeneous trapping of two immiscible liquids, one H_2O rich the other CH_4 rich.

4.4 Discussion

4.4.1 Chronology

The inclusion types observed occur isolated or in random clusters. No sharp inclusion trails indicative of trapping subsequent to mineral growth were observed. While no secondary inclusions are seen, it is still not easy to have a strict application of the concept of primary and secondary inclusions in the sense of Roedder (1984). This is especially complicated by the fact that the host mineral is spessartine, whose structural homogeneity means that it has no preferred orientation and may not easily define whether either set of inclusions is primary or secondary with respect to the others.

However, despite this apparent difficulty to establish which set of fluid inclusions is paragenetically older, it is still possible to identify cogenetic formation in the different fluid sets. The occurrence of Type 1 and Type 2 inclusions in the same cluster seems to suggest that H_2O-rich and CH_4-rich fluid inclusions were trapped at the same time. No evidence is available to suggest that Type 3 inclusions formed much later. It is possible then that the inclusions identified in the rocks of the Serra do Navio are all primary in origin, which formed at the same time and under roughly similar P – T conditions.

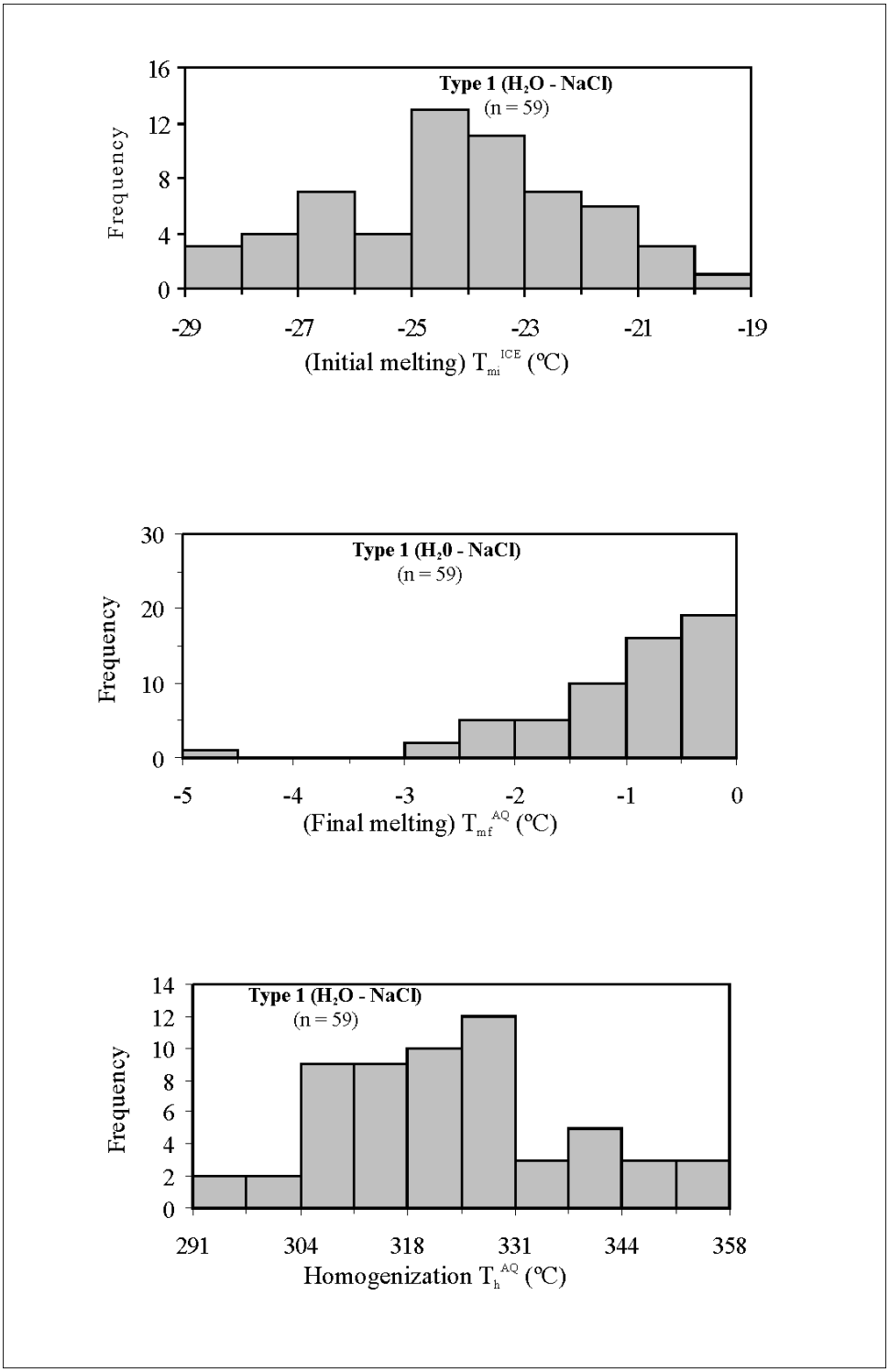

Fig. 4.4: Results of microthermometric studies for Type 1 inclusions represented in histograms. A: Temperatures of phase transitions with initial temperatures of melting (T_{mi}^{ICE}); B: Temperatures of phase transitions with final temperatures of melting (T_{mf}^{AQ}); C: Temperatures of phase transitions with temperatures of homogenization to the liquid phase ($T^{h\ AQ}$). In each case the total number of fluid inclusions studied is 59.

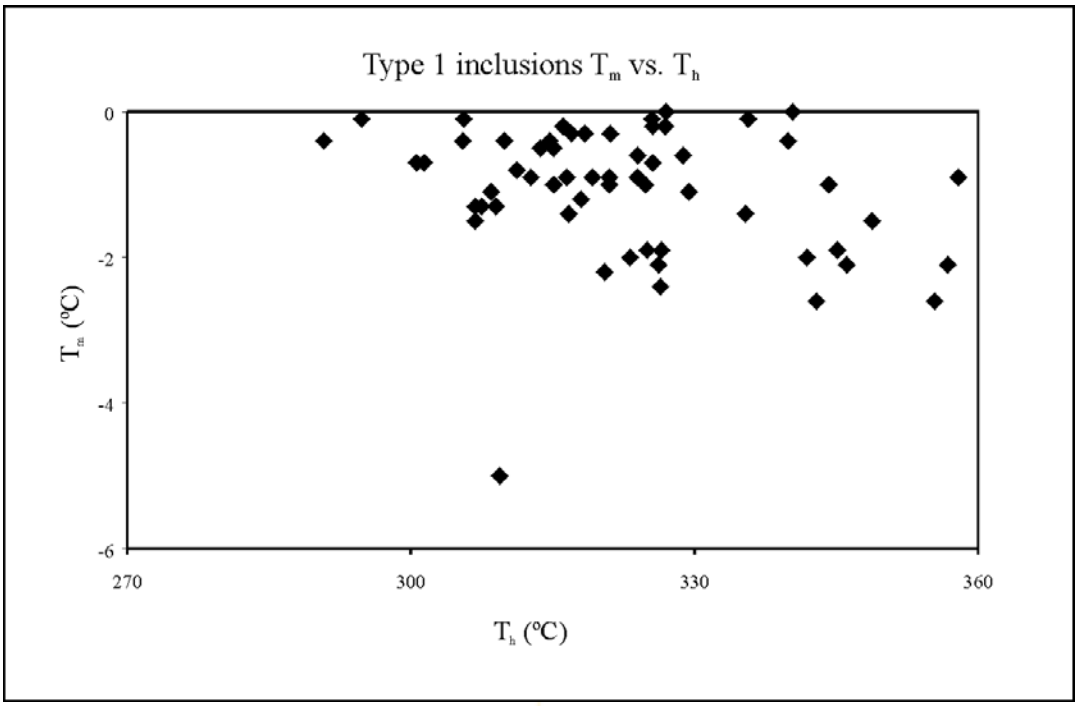

Fig. 4.5: Binary plot of the final melting temperatures plotted against homogenization temperatures of Type 1 inclusions (n = 59).

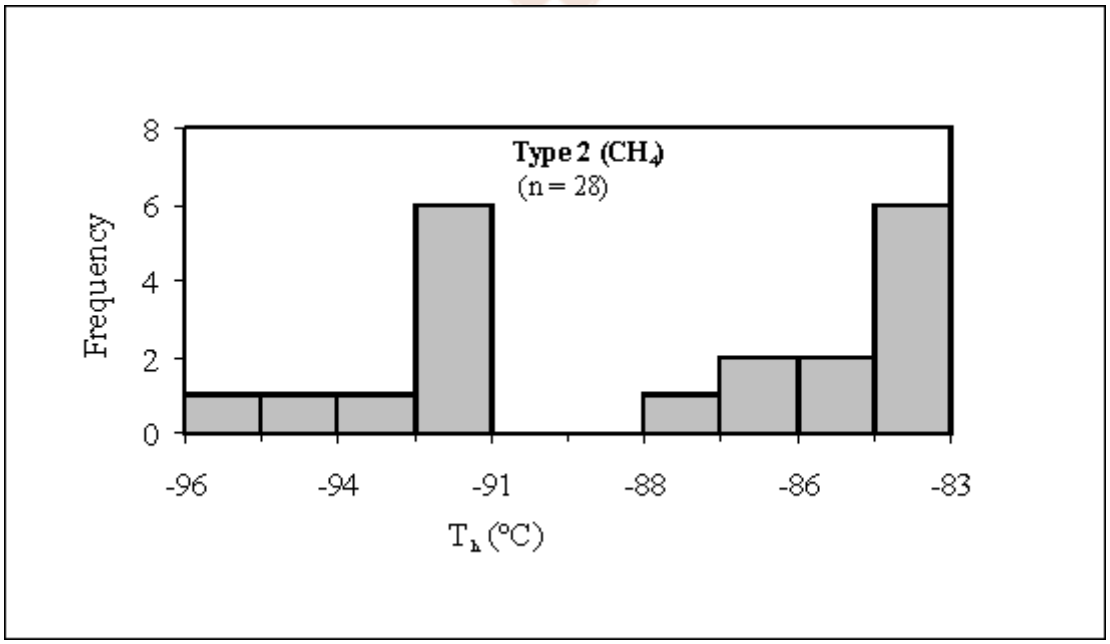

Fig. 4.6: Results of microthermometric measurements for Type 2 (CH_4) inclusions. Histogram depicts the homogenization temperature of methane to the liquid phase.

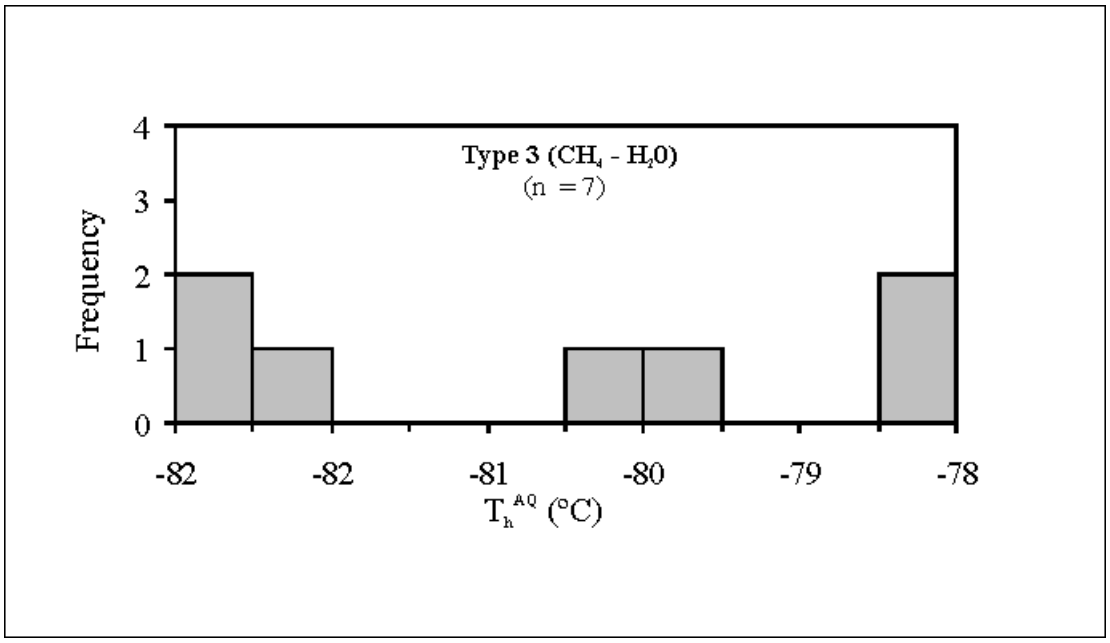

Fig. 4.7: Results of microthermometric examination of Type 3 (CH_4 – H_2O) inclusions. Histogram depicts the homogenization temperature of the mixed carbonic – aqueous inclusions to the liquid phase.

4.4.2 Fluid Separation

CH_4 and H_2O have very different physiochemical attributes, H_2O being dipolar and less volatile at room temperature and pressure whereas CH_4 is non polar but extremely volatile (Diamond, 2001). The result is that in the liquid state the mutual solubility of these two components is severely restricted. At very low temperatures two fluids are simultaneously stable, one rich in CH_4, the other in H_2O. This condition, called fluid immiscibility, results in coexistence of two fluid phases over a range of pressure – temperature – composition.

Three fluids were identified in inclusions in spessartine garnets from the Serra do Navio deposit, an aqueous rich phase (H_2O – NaCl), a carbonic phase (CH_4) and a mixed carbonic – aqueous phase (CH_4 – H_2O). Asserting that CH_4 and H_2O are immiscible and have been heterogeneously trapped, then it can be deduced that the original fluid was both methane and water rich. Then, by a process of *unmixing*, it produced a separate

carbonic phase as well as an aqueous phase. This is supported by the presence of the mixed aqueous – carbonic phase in minor amounts. Their presence may suggest that the process of unmixing was not efficient. It is, however, impossible to deduce the original composition of the individual components since their origin is heterogeneous. The original fluid is most possibly associated with graphite, which is widespread in the host rock and has been possibly derived from an organic source.

4.4.3 P – T conditions of entrapment

Entrapment temperature and pressure conditions can be estimated from the construction of isochores of both carbonic and aqueous inclusions (Roedder, 1984). The intersection of the isochores gives an accurate and reliable indication of the pressure and temperature of trapping. However, this technique is only applicable for homogeneously trapped inclusions. So in this study, the mixed carbonic – aqueous fluid inclusion type is not utilized in the estimation of entrapment conditions.

Isochores for aqueous inclusions (H_2O - NaCl) were calculated from the equation of state provided by Bodnar and Vityk (1994). The isochores for the carbonic inclusions (CH_4) were constructed from the Redlich-Kwong equation of state modified by Holloway (1981). These equations are adapted by Bakker (1999) in his software program *FLUIDS*.

For the Type 1 aqueous inclusions the homogenization temperatures T_h^{AQ} range between 291 ºC and 358 ºC (Fig. 4.8). The total salinity of NaCl is taken to be ~ 8 wt.%. Type 2 pure methane inclusions are depicted by isochores that range from –94.1 ºC to –83 ºC. These carbonic inclusions have an average molar volume between 57.3 cm^3/mol and 81.5 cm^3/mol, with corresponding densities between 0.28 g/cm^3 and 0.20 g/cm^3 respectively.

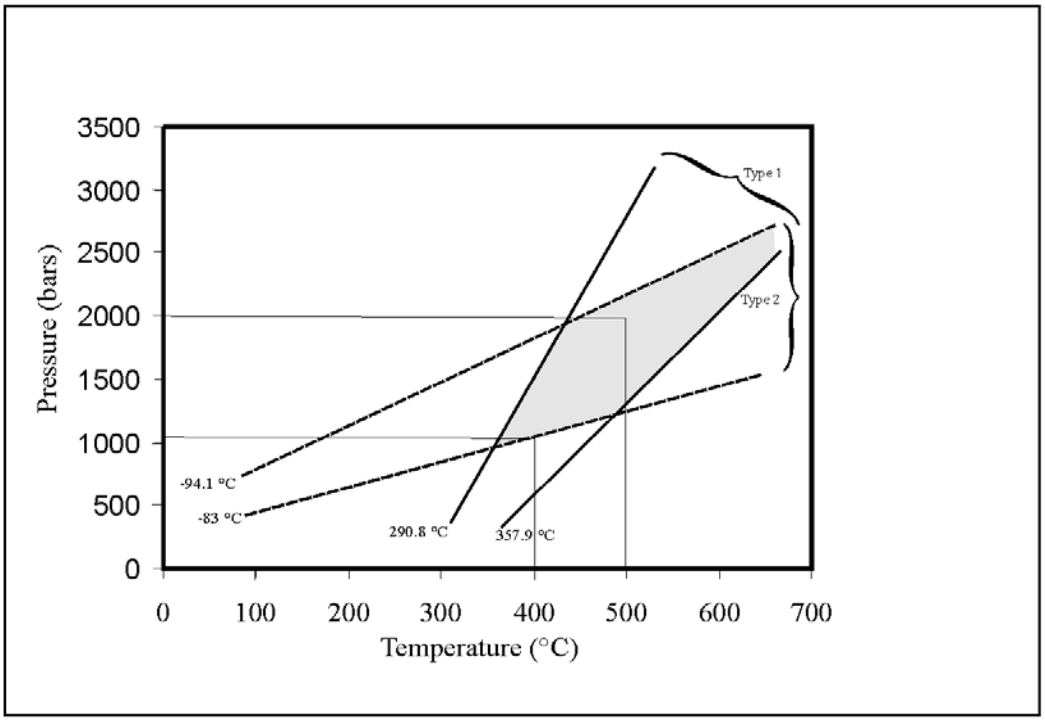

Fig. 4.8: Isochores for Type 1 and Type 2 inclusions. In each case the end members of homogenization temperatures are taken. The shaded light gray area indicates the intersection of this range and theoretically represents the possible P – T region of entrapment of the fluid inclusions.

The P – T conditions specified indicate a range of temperatures from 400 - ~ 800ºC and pressures between 1 – 3 kbar. This is not feasible given the composition of the lithologies (graphite and methane coexist only at temperatures < 500 ºC), the pressure and temperature of formation of the fluid inclusion host mineral (spessartine is a garnet stable at low temperature) and the extent of deformation of the enclosing lithology. It is, therefore, necessary to invoke post – trapping changes on the fluid inclusions as being responsible for this wide variation. Selective water leakage could be a possible post-trapping mechanism, even though petrographic features akin to this phenomenon were not observed. In granulites that contain some hydrous phase selective water leakage tends to offset the 'real' position of isochores (Touret, 2001).

The P – T constraints for the fluid compositions and fO_2 of CH_4 – H_2O and pure CH_4 inclusions give a temperature variation of 410 – 500 ºC, corresponding to pressures of 1.1 kbar and 2 kbar (Fig.4.8). At any depth the fluid pressure is a function of either lithostatic

pressure only, hydrostatic or both. If the fluid pressure is purely lithostatic (i.e. depth is a minimum) 1.1 kbar – 2 kbar corresponds to depth of ~ 4.2 to 5.7 km of metamorphism, assuming an average density of 2.7g/cm^3 for the overlying rock mass. Such a depth is proportional to geothermal gradients of 89.5 to 97.6 ºC/km

If, on the other hand, the fluid pressure is assumed to be hydrostatic (i.e. for maximum depth) then corresponding hydrostatic pressure would be represented by the relation:

$$P_{hydrostatic} = \lambda \cdot P_{lithostatic}$$

Where λ is the pore pressure gradient and is defined as $\lambda = \rho_{fluid}/\rho_{rock}$

Assuming a fluid density of 1g/cm^3 and a rock density of 2.7g/cm^3:

$$P_{lithostatic} = P_{hydrostatic} / \lambda$$

$$= (1.1 \sim 1.5)/2.7$$

$$= 3.0 – 4.05 \text{ kbars}$$

which corresponds to depths of 11 ~ 15 km.

No depth data from reconstructed stratigraphy is available, so whether the fluid pressure is close to lithostatic or hydrostatic conditions remains inconclusive. Such a depth range relates to a geothermal gradient of ~ 34 to 37 ºC/km which appears much more reasonable than the gradient for lithostatic pressure conditions. However, it is still considerably greater than geothermal gradients through today's upper continental crust. The only way to account for such high geothermal gradients is to assume that peak metamorphic conditions were reached during contact metamorphism. Scarpelli (1968 & 1973) has reported a sequence of metamorphic events that include contact metamorphism. Further, active tectonism including crustal shortening and thickening such as occurred in the area around the Serra do Navio deposit during the Trans-Amazonian orogeny, could also account for high geothermal gradients. However, the thicknesses of overlying rocks calculated for both lithostatic pressure (4.2 – 5.7km) and hydrostatic pressure (11 – 15 km) seems to be too high.

4.4.4 C – O – H Calculations

4.4.4.1 Introduction

Most metamorphic fluids can be described by three principle components: carbon, oxygen and hydrogen (the C – O – H system) (Huizenga, 2001). The C – O – H system is a fluid system essentially encompassing CO_2, CO, CH_4, O_2, H_2 and H_2O. Touret and Dietvorst (1983) have outlined a simplified profile to show that mixtures of these fluid species are present at various depths in the continental crust (Fig. 4.9). Various authors (e.g. Ohmoto and Kerrick 1977) have shown that this system can be used to delineate the compositions of crustal fluids as a function of pressure, temperature and oxygen fugacity. The ensuing model calculations have been used to describe such geologic processes as granulite genesis, fluid equilibria at low-grade metamorphic conditions as well as devolatization reactions in graphitic rocks (Huizenga, 2001). In this study, a calculation method devised by Huizenga (2003) is used to model the fluid inclusion composition.

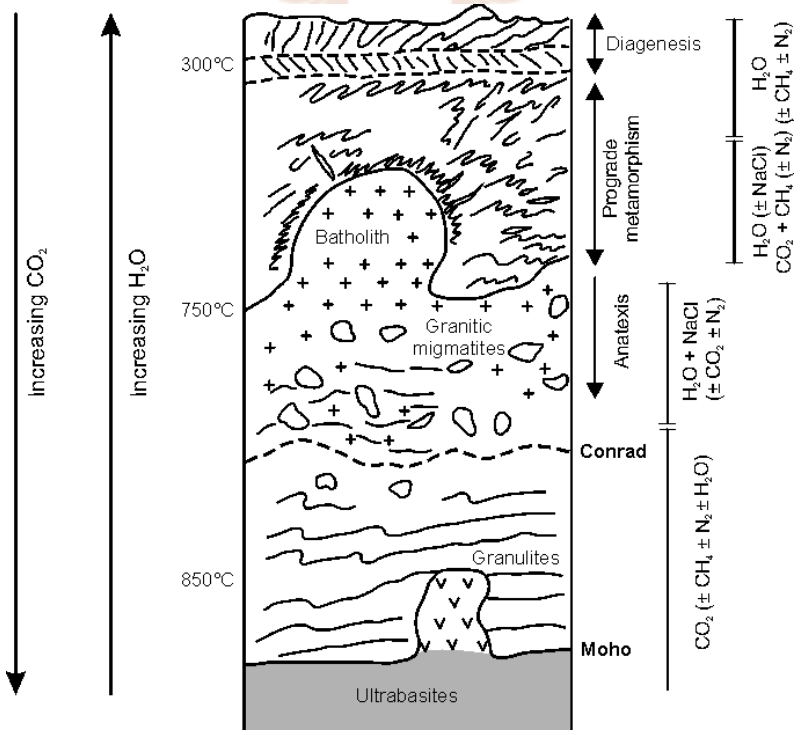

Fig. 4.9: Fluid distribution in the continental crust as inferred from fluid inclusion studies (after Touret and Dietvorst (1983)

4.4.4.2 Methods

Huizenga (2003) devised a fluid composition model for calculations in C-O-H fluid species that works on an *Excel* spreadsheet. This program works on the following suppositions:

(1) For any calculation, three input variables are required. The spreadsheet allows the following combinations:

- pressure, temperature and oxygen fugacity;
- pressure, temperature and the mole ratio $X CO_2/(X CO_2 + X CH_4)$;
- pressure, temperature and the atomic ratio H : O

These options are respectively determined by utilizing spreadsheets COH-1, COH-2 and COH-3 of the program.

(2) The calculations require the values of the fugacity coefficients of H_2O, CO_2, CH_4, and H_2 and CO. These can be selected from the tables supplied in the spreadsheet labeled H_2O, CO_2, CH_4, H_2 and CO. These were calculated after Shi and Saxena (1992).

(3) One must have a value for the carbon activity. If graphite is present, the carbon activity is unity; otherwise it is < 1.

(4) The program uses the fayalite-quartz-magnetite (FMQ) oxygen fugacity (fO_2) buffer, using the equation given by Ohmoto and Kerrick (1977) as a standard. The program allows the use different values for fO_2 by indicating deviations of the FMQ buffer (in $\log_{10}$ units).

To constrain the models thermodynamically, equations by Ohmoto and Kerrick (1977) as well as Shi and Saxena (1992) were used. All these equilibrium constants and fugacity coefficients are discussed by Huizenga (2003).

4.4.4.3 Results

For the purpose of the present study it is endeavored to constrain the composition of the fluid in the fluid inclusions assuming that the oxygen fugacity is buffered by fayalite-magnetite-quartz, FMQ. Additionally, the equilibrium composition of the immiscibly trapped fluid is determined.

The fluid composition for the given P (1000 and 2000 bars) T (400 and 500 ºC) and a carbon activity = 1, the composition is constrained using worksheet COH-1. The input and out put in each case are presented in Table 4.3

Worksheet COH-2 is used to calculate the equilibrium composition for the carbonic fluid phase that has a constant composition i.e. $XCH_4^{gas}=0.95$ *and* $XCO_2^{gas} = 0.05$. Input and output are summarized in Table 4.3 and 4.4.

Table 4.3: Input and output data for the calculation of the equilibrium composition of a carbon saturated C-O-H fluid of which at 1000 bar and 400°C.

Input		**Output**	
P_{fluid}	1000 bars	$\text{Log}_{10}\, fO_2^{\text{FMQ}}$	-29.1 bar
T	400 °C	$\text{Log}_{10}\, fO_2^{\text{fluid}}$	-29.5 bar
a_{carbon}	1.0	XH_2O	0.69
XCH_4^{gas}	0.95	XCO_2	0.30
XCO_2^{gas}	0.05	XCH_4	0.02
γH_2O	0.28	XH_2	$<10^{-3}$
γCO_2	1.06	XCO	0
γCH_4	1.55	$XCO_2/(XCO_2 + XCH_4)$	0.05
γH_2	1.40	X_0	0.22
γCO	1.56		

Table 4.6: Input and output data for the calculation of the equilibrium composition of a carbon saturated C-O-H at 2000 bar and 500°C.

Input		**Output**	
P_{fluid}	2000 bars	$\text{Log}_{10} fO_2^{FMQ}$	-24.1 bar
T	500 °C	$\text{Log}_{10} fO_2^{fluid}$	-25.0 bar
a_{carbon}	1.0	XH_2O	0.68
XCH_4^{gas}	0.95	XCO_2	0.30
XCO_2^{gas}	0.05	XCH_4	0.02
γH_2O	0.37	XH_2	0.01
γCO_2	1.75	XCO	0
γCH_4	2.37	$XCO_2/(XCO_2 + XCH_4)$	0.05
γH_2	1.69	X_0	0.22
γCO	2.29		

The results at the range of pressure and temperature are shown in Fig. 4.10 and 4.11. The figure shows that XH_2O and $\text{Log}_{10} fO_2^{fluid}$ are a function of $XCO_2/(XCO_2 + XCH_4)$. The XH_2O has a range from 0.72 – 0.74 at equilibrium conditions between corresponding P-T conditions of 1000 bar, 400 °C and 2000 bar 500 °C respectively. The fO_2 on the other hand ranges between -25.3 and -24.8 (Figs. 4.10 and 4.11)

It is evident that at P-T conditions of 1000bars and 400°C the fluid is dominated by water (XH_2O = 0.69) (Table 4.3). At 400°C and 200bars XH_2O = 0.68 (Table 4.4). In both cases XCO_2, XCH_4 and XCO are the same. The XH_2 is higher (0.01) at 500°C and 2000 bars than at 400°C and 1000 bars ($<10^{-3}$).

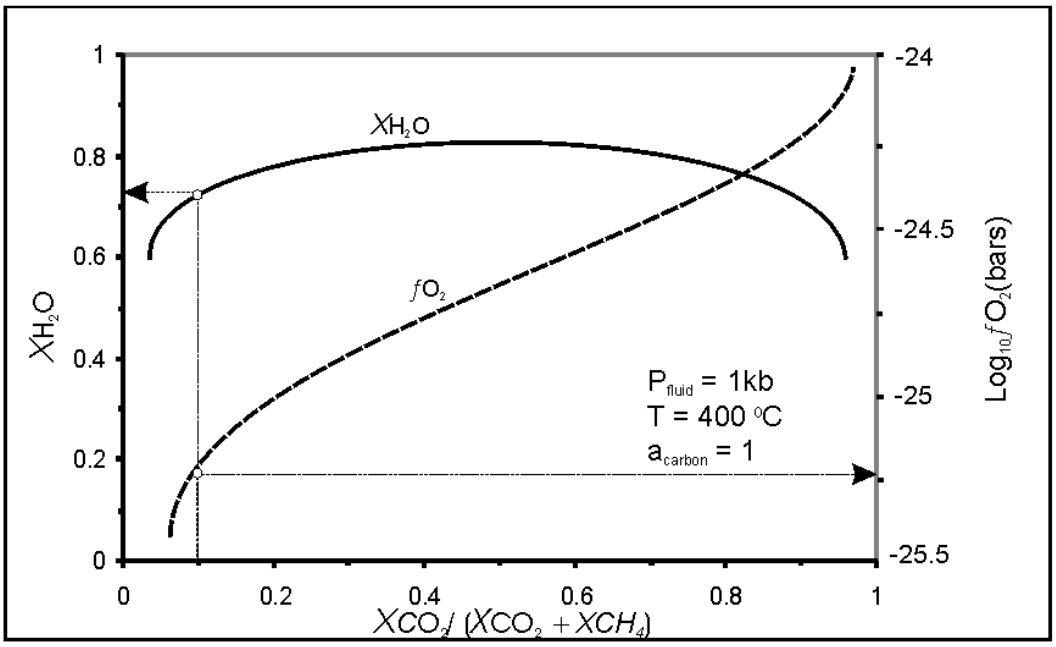

Fig: 4.10: Isobaric-isothermal diagram illustrating the variation of mole fraction of water (solid line) and oxygen fugacity (dashed line) for a carbon saturated C-O-H fluid. For a fluid of $X\mathrm{CO_2}/(X\mathrm{CO_2} + X\mathrm{CH_4}) = 0.1$ the typical $X\mathrm{H_2O}$ and fO_2 are shown.

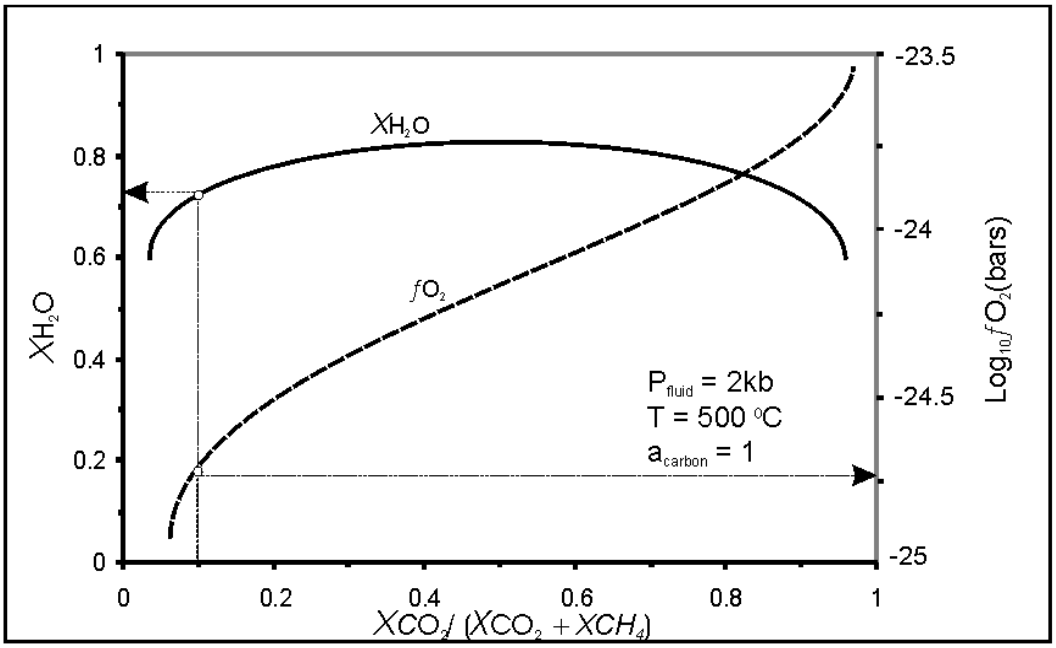

Fig: 4.11: Isobaric-isothermal diagram illustrating the variation of mole fraction of water (solid line) and oxygen fugacity (dashed line) for a carbon saturated C-O-H fluid. For a fluid of $X\mathrm{CO_2}/(X\mathrm{CO_2} + X\mathrm{CH_4}) = 0.1$ the typical $X\mathrm{H_2O}$ and fO_2 are shown.